GS and SGS Coherent Structures in Homogeneous Isotropic Turbulence

[O]**M. Ashraf Uddin**
Intelligent Modeling Laboratory, The University of Tokyo, 2-11-16 Yayoi, Bunkyo-ku, Tokyo 113-8656, Japan. E-mail: auddin@icebeer.iis.u-tokyo.ac.jp
Nobuyuki Taniguchi
Institute of Industrial Science, The University of Tokyo, 4-6-1 Komaba, Meguro-ku, Tokyo 153-8505, Japan. E-mail: ntani@iis.u-tokyo.ac.jp
Mamoru Tanahashi
Dept. of Mechanical and Aerospace Engineering, Tokyo Institute of Technology, 2-12-1 Ookayama, Meguro-ku, Tokyo 152-8552, Japan. E-mail: mtanahas@mes.titech.ac.jp
Toshio Miyauchi
Dept. of Mechanical and Aerospace Engineering, Tokyo Institute of Technology, 2-12-1 Ookayama, Meguro-ku, Tokyo 152-8552, Japan. E-mail: tmiyauch@mes.titech.ac.jp
Toshio Kobayashi
Institute of Industrial Science, The University of Tokyo, 4-6-1 Komaba, Meguro-ku, Tokyo 153-8505, Japan. E-mail: kobaya@iis.u-tokyo.ac.jp

Abstract: GS (grid-scale) and SGS (subgrid-scale) coherent structures in homogeneous isotropic turbulence are identified by a priori test. GS and SGS velocity fields are obtained by filtering the DNS velocity field for Re_λ =64.9 using two classical filters for LES: Gaussian filter and sharp cutoff filter, and the most important filter width is considered as the length of Kolmogorov microscale in the DNS field with a constant multiplication. Coherent structures in the GS field, i.e., structures larger than filter width are considered as grid-scale coherent structures and others are subgrid-scale coherent structures. Second invariant Q of the velocity gradient tensor is used for identification of these structures in GS and SGS fields. By visualizing the contour surfaces of second invariant Q, it is shown that GS and SGS fields itself contain lots of distinct tube-like coherent structures in homogeneous isotropic turbulence. The characteristic of GS and SGS coherent structures is somewhat similar to DNS structures, which indicates that the DNS field may contain multi-scale structures in turbulent flow.

1 INTRODUCTION

Direct numerical and large-eddy simulations (DNS and LES) have been widely used to study the physics of turbulence. However, direct numerical simulation for high Reynolds number flow requires formidable computing power, and is only possible for low Reynolds numbers. Generally, industrial, natural or experimental configurations involve Reynolds numbers that are far too large to allow direct numerical simulation, and the only possible method is large-eddy simulation.

Turbulent flow is completely nonlinear and complex and it has been shown in recent years that turbulent flows contain various types of vortical structures, more strictly coherent structures, but the lack of the proper knowledge about these structures prevents the development of turbulence theory and turbulent model. During the past decades, the studies on the coherent structures in turbulence have been the subjects of considerable interest among turbulence researchers. The study on these coherent structures is promising not only for understanding turbulence phenomena such as entrainment and mixing, scalar dissipation, heat and mass transfer, chemical reaction and combustion, drag and aerodynamic noise generation, but also for modeling of turbulence.

In the theoretical study, it is believed that tube-like structure is a type of eddy or vortex, which is the candidate of fine scale structure, particularly, in the small-scale motions in turbulence. [(1)(2)(3)(4)(5)] Nowadays, from direct numerical simulation of turbulence, [(6)(7)(8)(9)(10)(11)(12)(13)] fine scale tube-like coherent structures in homogeneous turbulence are observed, and the visualization of these small-scale structures in the turbulent flow becomes possible. In the recent studies, by direct use of local flow pattern, [(10)(11)] the cross-sections of tube-like coherent fine scale structures are investigated from DNS database of homogeneous isotropic turbulence in which the cross-sections are selected to include the local maximum of second invariant of the velocity gradient tensor on the axis of the fine scale tube-like coherent structures. In these studies, they have shown that mean diameter of the coherent fine scale structures is about 10 times of Kolmogorov microscale (h) and the maximum of mean azimuthal velocity is about a half of r.m.s of velocity fluctuations (u_{rms}) and that the Reynolds numbers dependence of these characters is very weak. The same analyses have been applied to turbulent mixing layer [(14)] and showed that the characteristics of tube-like coherent structures in homogeneous isotropic turbulence and fully developed turbulent mixing layer obey the same scaling law. Since the educed fine scale structures in their study have similar mean azimuthal velocity profiles and distinct axes, they described these structures as ‘coherent fine scale structures’ in turbulence. The characteristics of vortical structures in turbulent channel flows [(15)] and MHD turbulence [(16)] also show the similar behavior of tube-like structures in homogeneous isotropic turbulence. These results suggest that the existence of ‘coherent fine scale structure’ in turbulence is universal.

Although DNS is the most exact approach to turbulence simulation but too expensive and is possible relatively in simple flow fields while large-eddy simulation (LES) is less expensive and can simulate very complex flow fields in turbulence. With LES method, large-scale motion is directly calculated but small-scale needs to be modeled by subgrid-scale (SGS) model. Concerning the subgrid-scale model, it seems quite important to know what happened in the filtered field for LES from the actual turbulence including appearance or disappearance of the tube-like vortical structures in resolved or unresolved field.

Therefore, the purpose of this study is to filter DNS velocity field for obtaining the GS (grid-scale) and SGS (subgrid-scale) velocity fields in turbulent flow using classical filters for LES. Then we identify the grid-scale and subgrid-scale coherent structures and discuss the statistics of GS and SGS coherent structures in homogeneous isotropic turbulence.

2 LARGE-EDDY SIMULATION

2.1 DNS Data Base

In this study, DNS data of decaying homogeneous isotropic turbulence has been used, which is conducted by Tanahashi et al. [10] and is calculated by using 128^3 grid points. Reynolds number based on u_{rms} and Taylor microscale, l of the DNS data is Re_l =64.9.

2.2 GS and SGS Velocity Fields

To obtain the grid-scale (GS) and gubgrid-scale (SGS) velocity fields, we have directly filtered the above DNS velocity field using two classical filters: Gaussian filter and sharp cutoff filter for LES. In LES, a velocity component *u* can be decomposed into two components, one component is in the range of low wave-number of energy spectrum, large scale of motion, called GS component and is denoted by $\bar{u}$, and the other component is in the range of high wave-number of energy spectrum, small scale of motion, called SGS component and is denoted by u'. Their relation can be expressed as:

$$u = \bar{u} + u' \tag{1}$$

The filtering is represented mathematically in physical space as a convolution product. [17] The filtered part $\bar{u}$ of the variable *u* is defined formally by the relation:

$$\bar{u}(x) = \int_D G(x - x', \Delta)u(x')dx', \tag{2}$$

in which *G* is filter kernel function and Δ_i is the filter width in i-direction. The dual definition in the Fourier space can be obtained by multiplying the spectrum $\hat{u}(\mathbf{k})$ of *u*(x) by the spectrum $\hat{G}(\mathbf{k})$ of the kernel *G*(x) such that,

$$\hat{\bar{u}}(\mathbf{k}) = \hat{G}(\mathbf{k})\hat{u}(\mathbf{k}), \mathbf{k} = 0, \pm 1, \pm 2, \ldots\ldots\ldots \tag{3}$$

The function $\hat{G}$ is the transfer function associated with the kernel *G*.

2.3 Classical Filters for LES

In this study, two classical filters are used for performing the spatial scale separation. For a filter width Δ_i in i-direction, these filters in physical space (PS) and Fourier space (FS) are written as follows:

(I) Gaussian filter:

$$G(x_i) = \sqrt{\frac{6}{p\Delta_i^2}} \exp\left(\frac{-6x_i^2}{\Delta_i^2}\right) \qquad \text{(PS)} \tag{4a}$$

$$\hat{G}(k_i) = \exp\left\{-\frac{(\Delta_i k_i)^2}{24}\right\} \qquad \text{(FS)} \tag{4b}$$

(II) Sharp cutoff filter:

$$G(x_i) = 2\frac{\sin\left(\frac{px_i}{\Delta_i}\right)}{px_i} \qquad \text{(PS)} \tag{5a}$$

$$\hat{G}(k_i) = \begin{cases} 1, \left(|k_i| \le \dfrac{p}{\Delta_i}\right) \\ 0, \left(|k_i| > \dfrac{p}{\Delta_i}\right) \end{cases} \qquad \text{(FS)} \tag{5b}$$

Using the above two filters for LES in the Fourier space, one set of DNS data is filtered and the exact GS velocity field, $\bar{u}$ are obtained. After generating $\bar{u}$, we subtract the GS velocity field from DNS velocity field and obtain the SGS velocity field. That is, the SGS velocity field can be obtained by the relation (from Eq.1):

$$u' = u - \bar{u} \tag{6}$$

Filter width plays very important role with filter functions in this process. The characteristic filter width Δ_i is commonly used as the length, approximately proportional to the grid interval Δ in the previous researches. [18][19][20] The structures represented by the GS and SGS velocities consequently depend both on the grid interval and on the type of filter employed. In the previous studies, [10][11] it is shown that the mean diameter of the coherent fine scale eddy is about 10 times of Kolmogorov microscale (h) in turbulent flows. Therefore, in this study, the most important filter width, Δ_i, is considered as the length of Kolmogorov microscale in the DNS field with a constant multiplication. Since we are dealing with homogeneous isotropic turbulence, the filter width Δ_i is same in each direction and hereafter it is denoted by $\bar{\Delta}$.

2.4 Profiles of the DNS, GS and SGS Velocity Fields

In the previous study, [21] using several filter widths and different Reynolds numbers, it is shown that filter width $\bar{\Delta}$ depends on the Reynolds number of the flow, regardless of the filter employed. In this study, to obtain the GS and SGS velocity fields from DNS field for Re_l =64.9, we have considered filter width $\bar{\Delta}$ =10h, where h is obtained from the DNS velocity field. In order to understand the GS velocity field from the DNS velocity field, we compared DNS velocity with filtered velocity in Fig.1. For this purpose we have randomly chosen one-dimensional velocity profile in x_1 direction and have plotted $u_1(x_1)$ and $\bar{u}_1(x_1)$ for $\bar{\Delta}$ =10h in Fig.1. In all cases we

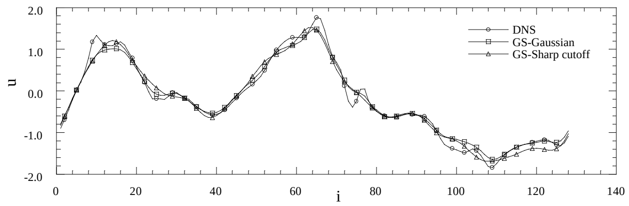

Fig. 1 Sample of filtered and unfiltered velocity fields.

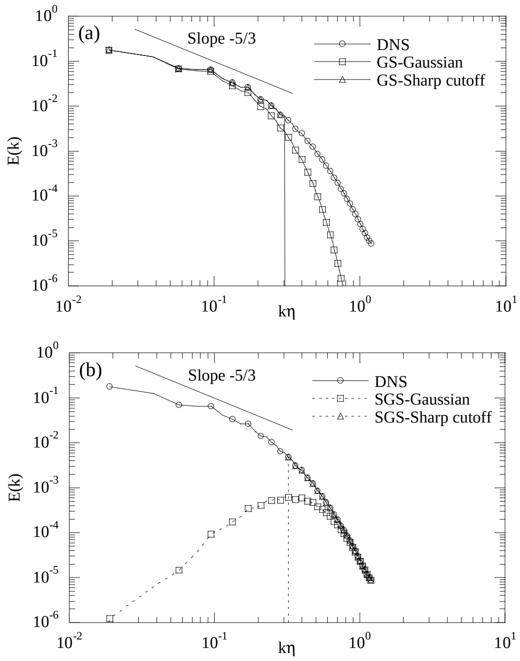

Fig. 2 Three-dimensional energy spectra of velocity fluctuations. (a) DNS and GS fields, (b) DNS and SGS fields.

obtained these one-dimensional profiles for the above two filter functions: Gaussian and sharp cutoff filter. Although $\overline{\Delta}=10h$ is a small value, but the profiles in Fig.1 suggest that the generation of GS velocity field as well as SGS velocity filed from this Re_l case is well using both filter functions.

Three-dimensional energy spectra of filtered and unfiltered velocity fluctuations for this filter width, $\overline{\Delta}=10h$ are presented in Fig.2, which is calculated by the definition written as follows:

$$E(k)=\sum_{k-\frac{1}{2}<|k|\le k+\frac{1}{2}} \frac{1}{2}\hat{u}(\mathbf{k})\hat{u}*(\mathbf{k}) \qquad (7)$$

In each case, the GS and SGS spectra are obtained by using Gaussian and sharp cutoff filter, and then compared with the DNS spectrum. The DNS spectrum shows the power decay close to $k^{-5/3}$. In the previous study, [(10)] using DNS database, it is shown that the energy dissipation rate is dominated by the fine scale eddies in homogeneous isotropic turbulence, which is beyond the discussion of this paper.

With the sharp cutoff filter, the SGS fields contain the velocity due to all the structures with wave number $|k|>p/\overline{\Delta}$. On the other hand, full range of wave numbers contributes to the SGS velocity in the case of Gaussian filter. Fig.2 reveals this difference in behavior for GS and

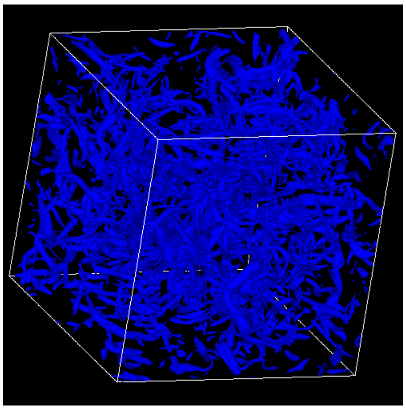

Fig. 3 Contour surfaces of the second invariant of the velocity gradient tensor (Q*=0.03) in the DNS field. Visualized region is the whole calculation domain. Second invariant is normalized by Kolmogorov microscale and r.m.s of velocity fluctuations.

SGS spectra using different filters for LES. This figure clearly indicates that, when sharp cutoff filter is used, the GS spectrum exactly collapsed with DNS spectrum in the range of low wave numbers ($|k|\le p/\overline{\Delta}$), while SGS spectrum is restricted in the high wave number range, and the contribution of subgrid scale is entirely due to the high wave numbers. The behavior of these spectra also confirms the accuracy of the filtering process. When Gaussian filter is used, the subgrid scales account for a fraction of the total (DNS) kinetic energy. Moreover, SGS energy has a significant contribution from the low wave numbers (i.e., the large scales) as we can see in Fig. 2(b). However, with this small $\overline{\Delta}$, it seems that GS fields contribute to the large part of energy dissipation rate for all filter functions.

3 GS AND SGS COHERENT STRUCTURES

In order to discuss about GS and SGS coherent structures, we notice the tube-like coherent fine scale eddy by visualization of flows in the DNS field. The concept usually associated with an eddy is that of a region in the flow where the fluid elements are rotating around a ‘set of points’. Identification of the eddy or vortex from DNS/LES database is a very difficult and complex task, requiring considerable computational efforts with proper identification method. There are several methods for identification of the vortical structures in turbulence with significant differences [(22)] and most of them show *threshold* dependence. As we discussed in the introduction, direct ‘local flow pattern’ [(23)] can educe coherent structures in several flow fields, [(10)(11)(12)(14)] which shows universal characteristics in turbulence. In our previous study, [(13)] using the above method we have identified the coherent fine scale eddies and its’ axes without using any thresholds and then discussed the spatial distribution of coherent fine scale eddies by visualization of axes in homogeneous isotropic turbulence. In this study, we use the same method to discuss about GS and SGS coherent structures in homogeneous isotropic turbulence.

Fig.3 shows the contour surfaces of normalized second invariant of the velocity gradient tensor Q in the DNS field for Re_l =64.9. The second invariant of the velocity gradient

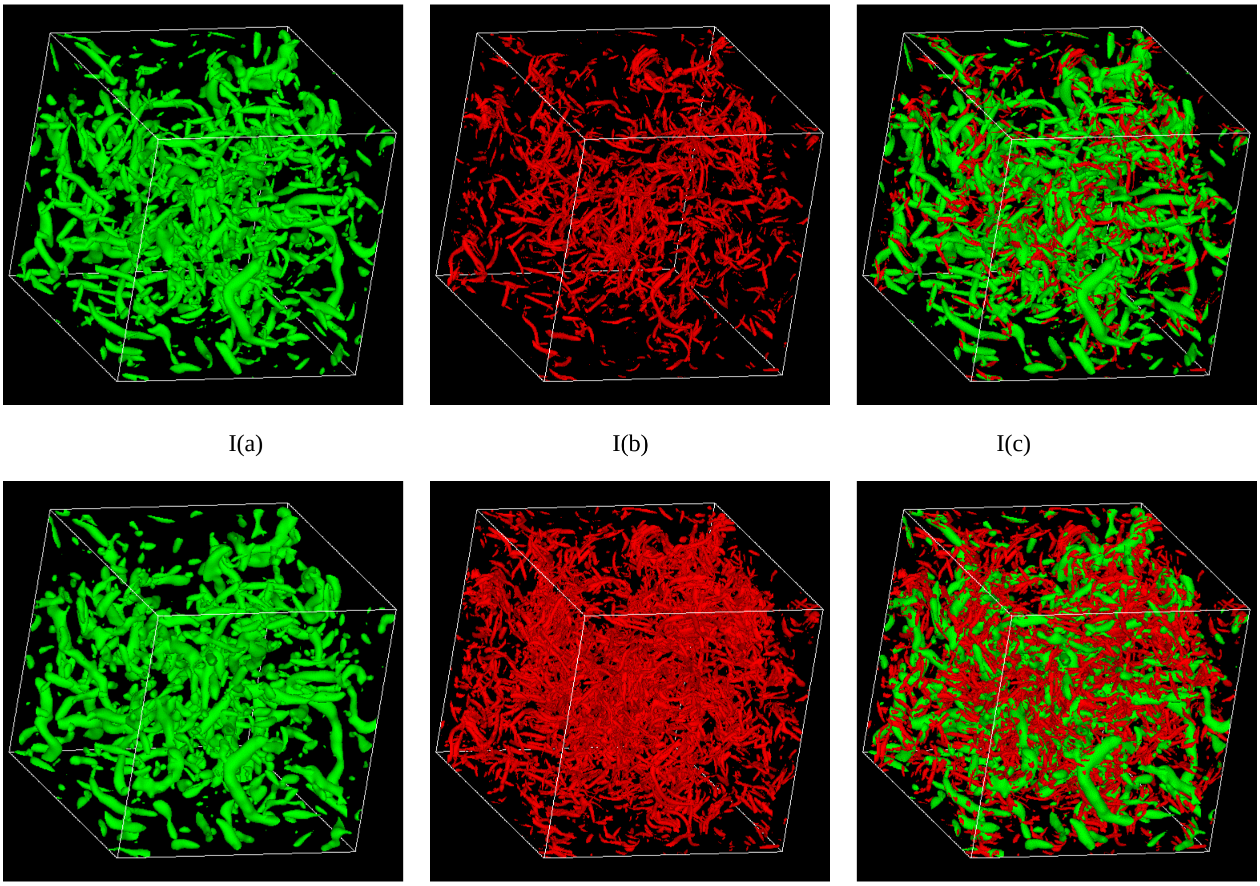

I(a) I(b) I(c)

II(a) II(b) II(c)

Fig. 4 Contour surfaces of the second invariant of the velocity gradient tensor in GS and SGS fields obtained from DNS field using (I) Gaussian filter and (II) sharp cutoff filter. Visualized region is same as in Fig.3. (a) GS field (Q*=0.02), (b) SGS field (Q*=0.01) (c) GS (Q*=0.02) & SGS (Q*=0.01) fields

tensor is defined as:

$$Q = -\frac{1}{2}\left(S_{ij}S_{ij} - W_{ij}W_{ij}\right), \tag{8}$$

where S_{ij} and W_{ij} are the symmetric and asymmetric part of the velocity gradient tensor A_{ij}. In Fig.3, the visualized region is whole calculation domain and the level of the isosurface is selected to be Q* =0.03. Hereafter, * denotes the normalization by Kolmogorov microscale h and root mean square of velocity fluctuations, u_{rms}, and for all cases h and u_{rms} are obtained from the DNS field. The normalization of Q by h and u_{rms} is due to the fact that the diameter and the maximum azimuthal velocity of tube-like fine scale structures can be scaled by h and u_{rms} [10] Fig.3 shows that lots of coherent tube-like structures are randomly oriented in homogeneous isotropic turbulence. However, if we increase or decrease the value of Q*, we can also show distinct tube-like structures in turbulence, little bit different from Fig.3, which means the visualization of fine scale structures significantly depends on the value of threshold of Q. [13]

Fig.4 shows the contour surfaces of second invariant of the velocity gradient tensor Q in GS and SGS fields obtained by using Gaussian and sharp cutoff filters with filter width $\overline{\Delta}=10h$. The visualized region and viewpoint in Fig.4 is same as in Fig.3 for all cases. The level of the isosurface for all cases in Fig.4 is selected to be Q* =0.02 for GS fields and Q* =0.01 for SGS fields. As we discussed above, the visualization of coherent structures depends on the threshold value of Q and we do not concern the strength of the structures, therefore, in this visualization we considered these different values for Q for different fields only to show the vortical structures in GS and SGS fields by visualization. Fig.4 clearly indicates that GS and SGS fields contain lots of distinct tube-like structures somewhat similar to DNS fields, which can best be defined as coherent structures or eddies in turbulence. [13] It is also clear that the size or length of GS structures in all cases seems to be larger than SGS structures.

It is known from the classical idea of fluid dynamics that several small-scale structure together form a large-scale structure, i.e., several small (SGS) structures entirely lie inside a large (GS) structure in the order of its size. However, Fig.4(c) clearly indicates that GS (green) and SGS (red) structures are quite distinct and unique in turbulence.

4. CHARACTERISTICS OF GS AND SGS COHERENT STRUCTURES

4.1 Identification Scheme

Since for visualization of flows in Figs.3-4, we use positive second invariant Q and we can see the existence of many tube-like coherent structures in DNS, GS and SGS fields in homogeneous isotropic turbulence. Obviously these tube-like structures contain at least one local maximum of Q on its' axis. With this local Q maximal, Tanahashi et al [10] have clarified the statistics of coherent fine scale structures in homogeneous isotropic turbulence. This method can best be used to study on the GS and SGS coherent structures in turbulence. Using this method, we can obtain a point on the cross-section on the axis of coherent structures with local Q maximum. The identification method consists of the following steps:

Step (a): Evaluation of Q at each collocation point from the results of DNS, GS and SGS fields.

Step (b): Probability of existence of positive local maximum of Q near the collocation points is evaluated at each collocation point from Q distribution. Because the case that a local maximum of Q coincides with a collocation point is very rare, it is necessary to define probability on collocation points.

Step (c): Collocation points with non-zero probability are selected to survey actual maxima of Q. Locations of maximal Q are determined within the accuracy of 10^{-6} in terms of relative error of Q by applying a 4th order Lagrange-interpolation polynomial to DNS, GS and SGS data.

Step (d): A cylindrical coordinate system (r, q, z) is considered by setting the maximal point as the origin. The z direction is selected to be parallel to the vorticity vector at the maximal point. The velocity vectors are projected on this coordinate and azimuthal velocity u_q is calculated.

Step (e): Point that has small variance in azimuthal velocity compared with the surroundings is determined. If the azimuthal velocities at r =1/5 computational grid space show same sign for all q, that point is identified as the center of the swirling motion.

Step (f): Statistical properties are calculated around the points.

4.2 Statistics of Coherent Structures

Figs.5-7 show the mean azimuthal velocity profile of coherent structures in DNS, GS and SGS fields for two filter functions. In these figures, r represents the radius of the coherent structures, which is determined by the distance between the center and the location where the mean azimuthal velocity reaches the maximum value. Mean azimuthal velocity profiles in all cases are normalized by $u_{\rm rms}$ and h, which are obtained from the DNS field. In Figs.5-7, symbols represent an azimuthal velocity of a Burgers' vortex, which is written as follows:

$$v_q = \frac{\Gamma}{2pr}\left[1-\exp\left(-\frac{ar^2}{4n}\right)\right], \qquad (9)$$

$$v_z = az\,, \qquad (10)$$

where G is the circulation of the Burgers' vortex tube and a is a stretching parameter. Using DNS database, [10][14] it was shown in the previous study that the mean azimuthal velocity profile of coherent fine scale structures in homogeneous isotropic turbulence and turbulent mixing layer could be approximated by a Burgers vortex. They [10]

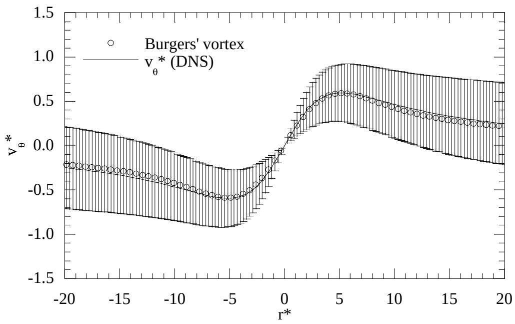

Fig. 5 Mean azimuthal velocity profile of the coherent structures in the DNS field, normalized by Kolmogorov microscale and r.m.s of velocity fluctuations. Symbols represent velocity profile of a Burgers' vortex and error bars denote variances of azimuthal velocity.

also have shown that the mean diameter of the coherent fine scale structures in homogeneous isotropic turbulence is about $10h$ and the maximum of mean azimuthal velocity is about half of $u_{\rm rms}$, and these characteristics of coherent structures are independent on Reynolds numbers of the flow. Fig.5 confirms these behaviors of the coherent structures for this Reynolds number case. Our interest is to discuss the characteristics of GS and SGS coherent structures comparing with the DNS results, hence, we have shown approximation of coherent structures in the GS and SGS fields with that of the Burgers' vortex in Figs.6-7.

The mean azimuthal velocity profile of GS-Gaussian coherent structures in Fig.6 (a) shows a good agreement with that of Burgers' vortex in the whole range as it as in DNS field. In Fig.7 (a), the agreement of mean azimuthal velocity profile for GS-sharp cutoff coherent structures with Burgers' vortex is good for relatively small distance (r*<$12h$), that is, the Burgers' vortex profile does not collapse with mean azimuthal velocity profile for the large distance. For Gaussian filter, the contribution of GS and SGS velocity fields are obtained from the whole region of DNS velocity field, while sharp cutoff filter separates the DNS velocity field in GS and SGS fields at the cutoff wave number. Maybe, that is one reason of these differences in Fig. 6(a) and 7(a). Moreover, filter size $\overline{\Delta}$ =$10h$ is relatively small. For large filter width, the large-scale structures, i.e., most of the coherent structures with large diameter accumulate in the GS field. Using large filter width, we have also seen (not shown) that the approximation of mean azimuthal velocity profile by Burgers' vortex becomes quite good for relatively large diameter tube like coherent structures in GS–sharp cutoff field as well as in GS-gaussian filed. On the other hand, although not in hole range, but Figs. 6(b) and 7(b) also show that the approximation of mean azimuthal velocity profile of SGS coherent structures in both SGS-Gaussian filed and SGS-sharp cutoff filed by Burgers, vortex is well in a certain range, and shows almost similar behavior for both filter functions. These results suggest that mean azimuthal velocity profile of coherent structures in LES can be approximate by that of a Burgers' vortex as well as in DNS.

The comparisons of normalized mean azimuthal velocity profile of coherent structures in DNS, GS and SGS

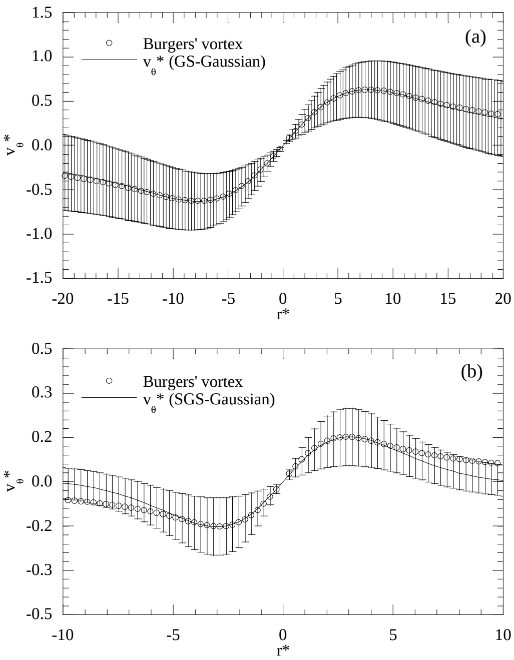

Fig. 6 Same as Fig.5, but (a) GS field and (b) SGS field obtained by using Gaussian filter.

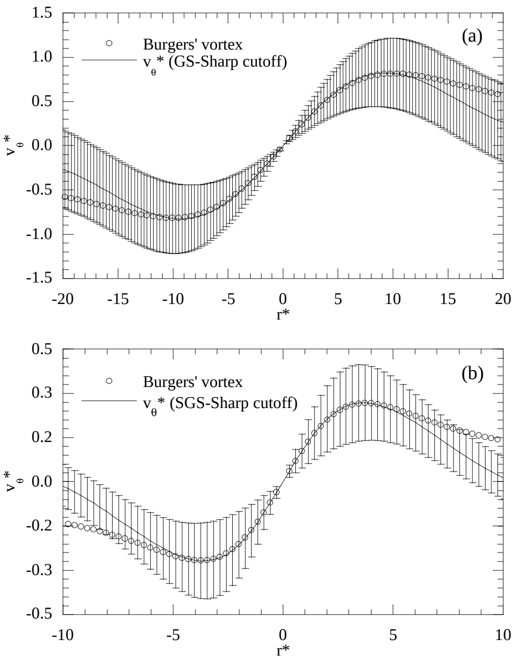

Fig. 7 Same as Fig.5, but (a) GS field and (b) SGS field obtained by using sharp cutoff filter.

fields for different filter functions are shown in Fig.8. Mean azimuthal velocity profile of GS structures for different filter functions with this filter width, $\overline{\Delta}$ collapse with DNS profile at r*=20h (Fig.8 (a)). On the other hand, mean azimuthal velocity profile of SGS structures for different filter functions collapse each other at r*=10h (Fig.8 (b)), but not with DNS profile. In all cases, the maximum of mean azimuthal velocity of GS structures is higher than DNS structures, and of SGS structures is lower than DNS structures. The maximum of mean azimuthal velocity and diameter of coherent structures are about $0.6u_{\mathrm{rms}}$ and $15h$ in

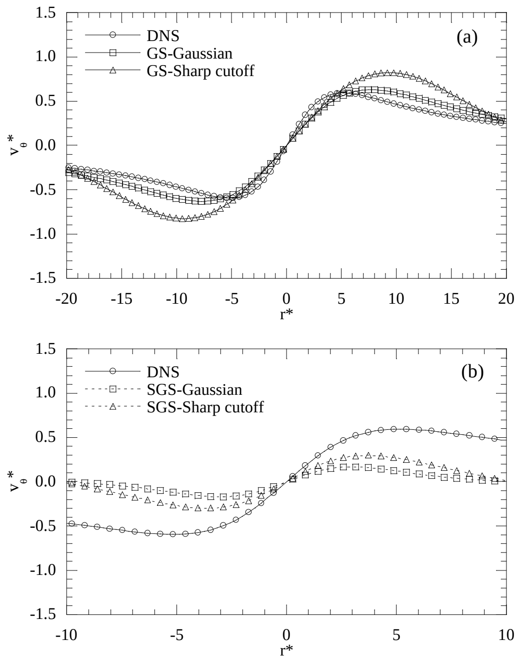

Fig. 8 Comparison of mean azimuthal velocity profile (v_q) of the DNS, GS and SGS coherent structures. (a) DNS and GS fields, (b) DNS and SGS fields. In all cases, mean azimuthal velocity profile is normalized by Kolmogorov microscale and r.m.s of velocity fluctuations obtained from DNS field.

GS-Gaussian field, and $0.8u_{\mathrm{rms}}$ and $20h$ in the GS-sharp cutoff field. On the other hand, the maximum of mean azimuthal velocity and diameter of coherent structures are about $0.2u_{\mathrm{rms}}$ and $5h$ in SGS-Gaussian field, and $03u_{\mathrm{rms}}$ and $7h$ in the SGS-sharp cutoff field. The maximum of mean azimuthal velocity for GS structures in the Gaussian field is close to the DNS field, but the maximum of mean azimuthal velocity for GS structures in the sharp cutoff field is larger than the DNS field. In actual LES, GS structures can be identified but SGS structures need to be model by SGS model. Coherent structures have high and thin energy dissipation regions around them and these regions contribute total energy dissipation in turbulence. [24] Since in SGS fields we can see the existence of coherent structures somewhat similar to DNS field, of course very small in size, this result is very worthy to develop a structures base SGS model for LES.

The probability density functions (pdf) of diameter of tube-like coherent structures in DNS, GS and SGS fields, which are normalized by h obtained from DNS field are shown in Fig.9 for different filter functions. It is clear that the peak of pdf of GS-structures in all cases do not coincide with each other or with DNS profile. Moreover, the peak of pdf of GS structure in the GS-sharp cutoff field shows higher value than in the GS-Gaussian field for this filter width. It is also revealed that the small diameter tube-like coherent structure in GS field is rare in all cases and large diameter of SGS structures reaches about $25h$. However, the collapse of pdf of diameter in the SGS fields is good, and the peak of pdf for SGS profile increases from the DNS profile for all filter functions.

Fig.10 shows the pdf of maximum of mean azimuthal velocity of coherent structures in the same DNS, GS and

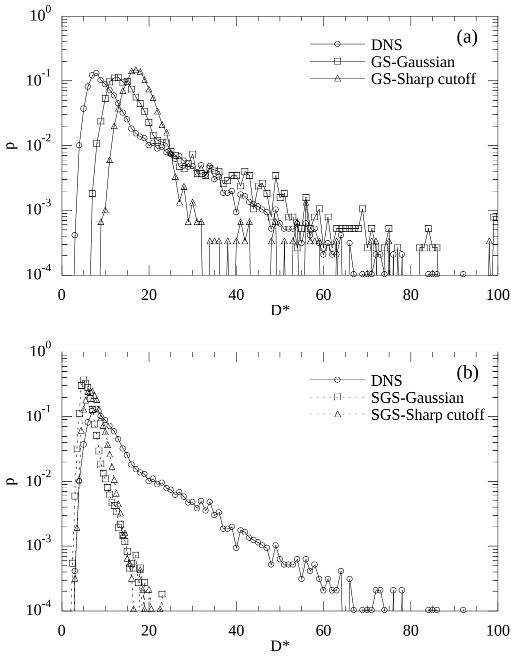

Fig. 9 Probability density function of diameter of coherent structures normalized by Kolmogorov microscale. (a) DNS and GS fields, (b) DNS and SGS fields.

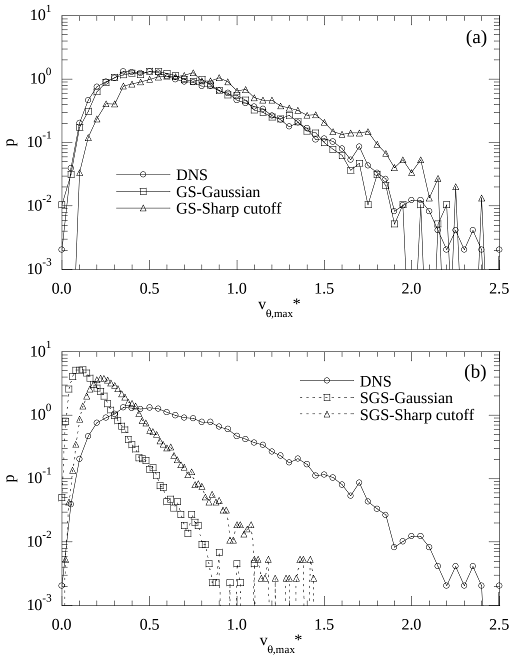

Fig. 10 Probability density function of the maximum of mean azimuthal velocity of coherent structures normalized by r.m.s of velocity fluctuations. (a) DNS and GS fields, (b) DNS and SGS fields.

SGS fields using different filter functions, which is normalized by u_{rms}. It is revealed that, GS-Gaussian profile collapse with DNS profile well in the whole range. The profile in the GS-sharp cutoff field is smaller than DNS profile at small azimuthal velocity and larger than that at large azimuthal velocity of the tube-like coherent structures. The maximum value of mean azimuthal velocity in GS and DNS fields seems to be same. On the other hand, SGS profiles of mean azimuthal velocity for both filter functions do not coincide each other or with DNS profile. The maximum value of mean azimuthal velocity profile is lower than $1.5u_{rms}$, i.e., about half of DNS value. Using large and different filter width, we have seen (not shown) that the pdf of SGS profile becomes very close with DNS profile and the maximum value in the SGS filed never exceed the maximum value in the DNS field. That is, the characteristics of GS and SGS coherent structures significantly depend on the filter widths. This behavior is interesting to study on the coherent structure in actual LES or to develop some LES modeling based on the coherent structures in turbulence. In the previous study, [(10)(14)] it was shown that the coherent fine scale structures could be scaled by Kolmogorov microscale and r. m. s of velocity fluctuations. The above results in the present study also suggest that the GS and SGS coherent structures may possible to scale by h and u_{rms} as well as in DNS.

5 CONCLUSIONS

In this study, GS and SGS coherent structures in homogeneous isotropic turbulence are identified. The GS and SGS velocity fields are obtained by filtering the DNS velocity field using classical filters for LES. By visualizing the contour surfaces of second invariant Q in GS and SGS fields as well as in DNS field, it is shown that GS and SGS fields itself contain lots of distinct tube-like coherent structures in homogeneous isotropic turbulence, which indicates that the DNS field contain multi-scale structures in turbulent flow. The characteristics of these GS and SGS coherent structures are somewhat similar to DNS coherent structures. These GS and SGS coherent structures can be scaled by h and u_{rms} as well as in DNS.

6 REFERENCES

(1) Townsend, A. A., “On the fine-scale structure of turbulence”, Proc. R. Soc. Lond., A208(1951), pp. 534-542.

(2) Tennekes, H., “Simple model for the small-scale structure of turbulence”, Phys. Fluids, 11(1968), No. 3, pp. 669-671.

(3) Lundgren, T. S., “Strained Spiral Vortex Model for Turbulent Fine Structure”, Phys. Fluids, 25(1982), pp. 2193-2203.

(4) Pullin, D. I. and Saffman, P. G., “On the Lundgren-Townsend Model of Turbulent Fine Scales”, Phys. Fluids, A5(1993), pp. 126-145.

(5) Saffman, P. G. & Pullin, D. I., “Anisotropy of the Lundgren-Townsend Model of Fine-scale Turbulence”, Phys. Fluids, A6(1994), pp. 802-807.

(6) She, Z. –S., Jackson, E. and Orszag, S. A., “Intermittent Vortex Structures in Homogeneous Isotropic Turbulence”, Nature, 344(1990), pp. 226-228.

(7) Vincent, A. and Meneguzzi, M., “The spatial structure and statistical properties of homogeneous turbulence”, J. Fluid Mech., 225(1991), pp. 1-20.

(8) Jimenez, J., Wray, A. A., Saffman, P. G. and Rogallo, R. S., “The Structure of Intense Vorticity in Isotropic Turbulence”, J. Fluid Mech., 255(1993), pp. 65-90.

(9) Vincent, A. & Meneguzzi, M., “The dynamics of

vorticity tubes in homogeneous turbulence", J. Fluid Mech., 258(1994), pp. 245-254.
(10) Tanahashi, M., Miyauchi, T. and Ikeda, J., "Scaling law of coherent fine scale structure in homogeneous isotropic turbulence", Proc. of 11th Symp. on Turbulent Shear Flows. 1(1997), pp. 4-17-4-22 .
(11) Tanahashi, M., Iwase, S., Uddin, M. A. and Miyauchi, T., "Three dimensional features of coherent fine scale eddies in turbulence", Turbulence and Shear Flow Phenomena-1 1st Int. Symp., Santa Barbara, California, Sep. 12-15(1999)., pp. 79-84.
(12) Tanahashi, M., Uddin, M. A., Iwase, S. & Miyauchi, T., "Three dimensional feature of coherent fine scale eddies in homogeneous isotropic turbulence", Trans. JSME, 65-B(1999), No. 638, pp. 3237-3243.
(13) Uddin, M.A., Tanahashi, M., Iwase, S. and Miyauchi, T., "Visualization of Axes of Coherent Fine Scale Eddies in Homogeneous Isotropic Turbulence", the 3rd Paci. Symp. on Flow Visualization and Image Processing (PSFVIP-3), Maui, Hawaii, March.18-21, CD-ROM Proc., C3-2(2001), No. F3204.
(14) Tanahashi, M., Miyauchi, T. and Matsuoka, K., "Coherent fine scale structures in temporally developing turbulent mixing layers", Proc. 2nd Int. Symp. on Turbulence, Heat and Mass Transfer, Vol. 2(1997), pp 461-470.
(15) Tanahashi, M., Das, S. K., Shoji, K. and Miyauchi, T., "Coherent fine scale structure in turbulent channel flows." Trans. JSME, Vol. 65-B(1999), No. 638, pp. 3244-3251.
(16) Tanahashi, M., Tsujimoto, T, Karim, M. F., Fujimura, D. and Miyauchi, T., "Anisotropy of MHD homogeneous turbulence". Trans. JSME, Vol. 65-B(1999), No. 640, pp. 3884-3890.
(17) Leonard, A. "Energy Cascade in Large-eddy Simulations of Turbulent Fluid Flows", Adv. in Geophys., 18A(1974), pp. 237-248.
(18) Piomelli, U., Yu, Y. and Adrian, R. J., " Subgrid-scale Energy Transfer and Near-wall Turbulence Structure", Phys. Fluids, 8(1) (1996), pp. 215-224.
(19) Piomelli, U., Moin, P. and Ferziger, J. H., " Model Consistency in Large Eddy Simulation of Turbulent Channel Flows", Phys. Fluids, 31(7)(1988), pp. 1884-1891.
(20) Horiuti, K., "A Proper Velocity Scale for Modeling Subgrid-scale Eddy Viscosities in Large Eddy Simulation", Phys. Fluids A5(1)(1992), pp.146-157.
(21) Uddin, M.A., Tanahashi, M., Nobuyuki, T., Iwase, S. and Miyauchi, T., "Grid-scale and Subgrid-scale Eddies in Turbulent Flows ~ a Priori Test", the 4th Int. Conf. on Mech. Eng. (ICME2001), Dhaka, Bangladesh, Dec. 26-28(2001), in press.
(22) Jeong, J. and Hussain, F., "On the Identification of a Vortex", J. Fluid Mech., 285(1995), pp. 69-94.
(23) Chong, M.S., Perry, A.E. and Cantwell, B.J., "A General Classification of Three-dimensional Flow Fields", Phys. Fluids A2(1990), pp. 765-777.
(24) Tanahashi, M., Miyauchi, T. & Yoshida, T., "Characteristics of small scale vortices related to turbulent energy dissipation", Transport Phenomena in Thermal Fluid Engineering, Vol. 2(1996), pp. 1256-1261.